

# JL-2: A Mobile Multi-robot System with Docking and Manipulating Capabilities

Wei Wang<sup>1</sup>, Wenpeng Yu and Houxiang Zhang<sup>2</sup>

<sup>1</sup>Robotics Institute, Beihang University, Beijing, China

<sup>2</sup>TAMS, Department of Informatics, University of Hamburg, Hamburg, Germany  
 wangweilab@buaa.edu.cn

**Abstract:** *This paper presents a new version of the JL series reconfigurable multi-robot system called JL-2. By virtue of the docking manipulator composed of a parallel mechanism and a cam gripper, every mobile robot in the JL-2 system is able to not only perform tasks in parallel, e.g. moving and grasping, but also dock with each other even if there are large misalignments between two robots. A motorized spherical joint is formed between two docked robots to enhance the locomotion capability of JL-2. To fulfill the demands of reconfiguration, a distributed control system and sonar based docking guidance system are designed for the JL-2 prototype. Based on the above design, the JL-2 prototype has been built and successfully demonstrated to confirm the validity and functionality of the proposed capabilities.*

**Keywords:** *Reconfigurable robot, Mobile robot, Docking mechanism, Manipulator, Distributed control*

## 1. Introduction

Self-reconfiguration technology is expected to be one of the key answers of how to combine flexibility, robustness, ability to self-repair and all-terrain navigation in one mobile robot system (Mondada, F.; et al., 2003), which will serve for applications like space explorations (Visentin, G.; et al., 2001), rescue (Casper, J.; Murphy, R.R., 2000) or civil exploration (Hirose, S.; Morishima, A., 1990). For a self-reconfigurable mobile robotic system, besides the communication among robots, an innovative cooperation is achieved by self-reconfiguration, that is, the capability to actively connect and disconnect, and to adjust the postures of the robots to enhance their locomotion abilities in the connected state. Furthermore, by dividing a mobile reconfigurable robot system into several smaller units, explorations in large areas can be performed in parallel to keep high efficiency.

From the authors' viewpoint, the following characteristics may ensure the above advantages of a self-reconfigurable mobile multi-robot system: 1) Docking ability tolerating the aligning errors introduced by the rugged terrains in the field; 2) Posture-adjusting ability with three active DOFs between robots when docked; 3) Independent navigation and manipulation capabilities integrated in every single robot.

From 2004 to now, we have been developing the JL series based on the above ideas. As the first version, JL-1 features a powerful posture-adjusting mechanism with three DOF (Zhang, H.X.; et al., 2006), as well as limited docking ability in flat terrains (Wang, W.; et al., 2008). The new version JL-2 is based on but distinguishes from its predecessor JL-1 in two aspects: 1) Docking ability tolerating the aligning errors in five dimensions which is

induced by the rugged terrains; 2) Docking manipulator integrating the docking mechanism and manipulability on each robot.

In this paper, after the survey of the related work, the design ideas are summarized as the basis of the prototype realization. The mechanical structure of JL-2 is designed according to the design ideas. One robot in the JL-2 system is composed of several units, among which the docking manipulator endows JL-2 with the docking and grasping capabilities. Besides the kinematics, the control system of the JL-2 system is also developed for the autonomous reconfiguration. The grasping, docking, and posture-adjustment functions are also analyzed in detail based on the kinematics of the docking manipulator and the spherical joint between two docked robots. After that, a series of tests are presented to prove the capabilities of JL-2. In the end, the conclusions are given.

## 2. Related Work in Literature

To negotiate the rugged terrains in the outdoor environment, different kinematic structures are designed for the rescue or surveillance robots. For example, Packbot (Matthies, L.; et al., 2000) and Inuktun Micro VGTV (Murphy, R. R., 2000) are shape-changing tracked robots; CUL robot (Tokuda, K.; et al., 1999) and Shrimp (Estier, T.; et al., 2000) adopt the wheel types; ACM-R3 (Mori, M.; Hirose, S., 2002) and Perambulator (Lu, Z. L.; et al., 2006) are snake robots; Souryu (Masam, A.; et al., 2004), MOIRA (Haraguchi, R.; et al., 2005) and OT (Borenstein, J.; et al., 2007) belong to the multi-segments robot. Though these robots adapt well to the expected terrains, it is difficult for them to overcome the obstacles beyond their capabilities. The mobile robotic system

being able to reconfigure according to the change of the environment may be more robust and efficient in the complex and unknown environment (Yim, M.; et al., 2007).

Compared with the Lattice and Chain/Tree Modular Self-configurable Robots (MSRs), the mobile MSR is more suitable to move and manipulate in the outdoor terrains. However, before it is available in real works, the mobile MSR should be improved to realize docking on fields, 3-D posture-adjusting and manipulating.

Up to date, different docking mechanisms are applied in the MSRs. The magnetic force based docking mechanism is only suitable for the Lattice and Chain/Tree MSRs, whose modules are relatively simple and light, such as Miche (Gilpin, K.; et al., 2008), Molecubes (Zykov, V.; et al., 2005), M-TRON I (Murata, S.; et al., 2002), etc. But for a Mobile MSR, it is difficult to take advantage of the magnetic docking method because the weight of one module is much bigger than that of the other two MSRs due to its self-contained mobile capability. Some latch docking mechanisms (Nilsson, M., 2002), (Sproewitz, A.; et al., 2008) are characterized by the self-aligning and holding properties, which are helpful to realize robustly docking when there are large disalignments between two robots.

Two typical Mobile MSRs are Millibot (Brown, H.B.; et al., 2002) and SWARM-bot (Mondada, F.; et al., 2004), (Gross, R.; et al., 2006). Although these two prototypes feature independent mobility of modules and relative high adaptability to the rugged terrains after docked, they still suffer from the limited DOF of the posture-adjusting mechanism as well as the strict docking conditions. When docked, the Millibot robots can only lift or lower each other, but they are not capable of effecting rotation and yawing movements. With SWARM-bot, the situation is similar, except that the distance between two docked robots can be adjusted by the reconfiguration mechanism. This is due to the difficulty of integrating a powerful active three DOFs posture-adjusting mechanism into the limited space of one module.

When the manipulating capability are taken into account, some cooperative robots systems are attractive, since they are not only able to connect and disconnect autonomously, but their single units are also capable of manipulation. Gunryu (Hirose, S.; et al., 1996) and CEBOT (Kawauchi, Y.; et al., 1994) are all composed of mobile platforms with serial manipulators. The transformable wheel of the SMC rover (Kawakami, A.; et al., 2002) can be considered as a simple mobile robot consisting of one wheel and a multi-functional manipulator which can grasp objects or connect the wheel with the central platform or other wheels. In these prototypes, the docking actions are performed by the manipulators. But the joints between two connected robots cannot change the robot's posture arbitrarily because of the limited output torques instinctively provided by their serial structures.

Based on the known technologies and the results of JL-1, JL-2 is developed to integrate the robustly docking and manipulating capabilities together. The focus of this paper is to introduce the theories and realization of JL-2 to fulfill the three requirements in section 1.

### 3. Kinematics Design and Realization

#### 3.1. System overview and design ideas

The new design of the JL-2 prototype is based on the following ideas:

1. *Combining the manipulation and a part of the docking and posture-adjusting functions to form a docking manipulator.* One robot can take advantage of its manipulator to grasp and operate objects independently, as well as to connect with another robot in the system. Moreover, the joints of the manipulator also provide the DOF for the posture-adjusting and docking procedures.
2. *Grasping-locking and gradual-alignment docking procedure.* To simplify the structure of the docking mechanism, the docking procedure will be divided into different stages. At the beginning of docking, the gripper will surround and grasp the connector of another robot to prevent it from escaping from the docking area. In the following stages, only one or two misalignments will be diminished one by one.
3. *Self-assembling motorized spherical joint for the posture-adjusting mechanism.* This design distributes the three DOF of the posture-adjusting mechanism to different robots. The joint is only fully functional when two robots are connected.

Based on the above ideas, the JL-2 prototype is designed, as shown in Fig. 1. As same as JL-1, JL-2 is also composed of three independent robots with full navigation abilities in the field. They are called the back robot, the middle robot and the front robot respectively. If the robots connect, they will form a chain structure in which one robot is able to actively adjust the posture of the adjacent one in three dimensions by virtue of the two spherical joints between them.

One robot in JL-2 may consist of three units: two track units, one rotation unit and a docking manipulator. In fact, for economical reasons only the middle robot

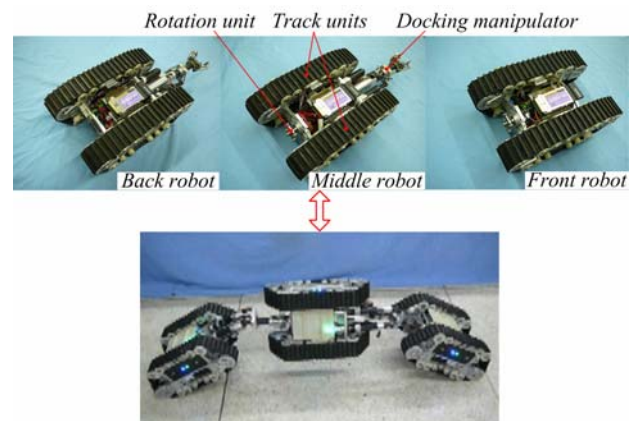


Fig. 1. Three robots in the JL-2 system

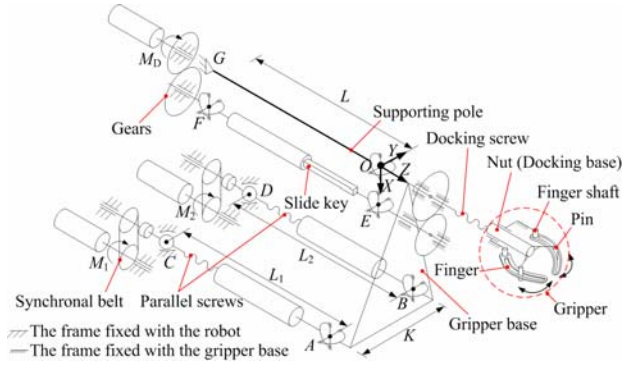


Fig. 2. Kinematic diagram of the docking manipulator

contains all of these units. Though it is ideal to construct all of the robots with a uniform structure, currently a simplified version is sufficient for testing the basic functions of JL-2.

### 3.2. Docking manipulator

The functions of the docking manipulator include: 1) Grasping and manipulating objects; 2) Holding the docking disk of the rotation unit on the other robot; 3) Adjusting the pitching and yawing postures between two connected robots.

Fig. 2 shows the kinematic structure of the docking manipulator, which is composed of a two-DOF parallel mechanism and an end gripper. The parallel mechanism consists of two parallel ball screws  $AC$  and  $BD$ , the gripper base  $ABO$ , and the supporting pole  $GO$  fixed with the robot platform. There are two ball bearings at points  $C$  and  $D$ , and three hooker joints at points  $A$ ,  $B$  and  $O$  respectively. Along with the changes of the two screws' lengths, namely  $L_1$  and  $L_2$ , the gripper base will turn around the axes  $X$  and  $Y$ . Equations (1) and (2) show the relations between  $L_1$ ,  $L_2$  and the yawing and pitching angles  $\theta_x$ ,  $\theta_y$ .

$$L_1 = (\mathbf{L}^2 + 4\mathbf{K}^2 + 2\mathbf{K}\mathbf{L}s\theta_y + 2\mathbf{K}^2c\theta_x - 2\mathbf{K}^2c\theta_y + 2\mathbf{K}\mathbf{L}s\theta_xc\theta_y + 2\mathbf{K}^2s\theta_xs\theta_y)^{1/2} \quad (1)$$

$$L_2 = (\mathbf{L}^2 + 4\mathbf{K}^2 + 2\mathbf{K}\mathbf{L}s\theta_y - 2\mathbf{K}^2c\theta_x - 2\mathbf{K}^2c\theta_y - 2\mathbf{K}\mathbf{L}s\theta_xc\theta_y - 2\mathbf{K}^2s\theta_xs\theta_y)^{1/2} \quad (2)$$

Where,

$L$  is the distance between the main hooker joint and the center of the ball bearing along the  $Z$  axis;

$K$  is half the distance between the two hooker joints supporting the ball screws;

$s$  and  $c$  are the abbreviations of  $\sin$  and  $\cos$  respectively.

The gripper fixed on the gripper base consists of a screw-nut mechanism and two fingers which can rotate around two shafts respectively. Two pins are fixed with the nut (Docking base) and pass through the grooves of the fingers called the cam grooves. When the docking screw is turning, the pins will move forward or backward and drive the gripper to close or open by virtue of the special shape of the cam groove. To arrange the mass center of

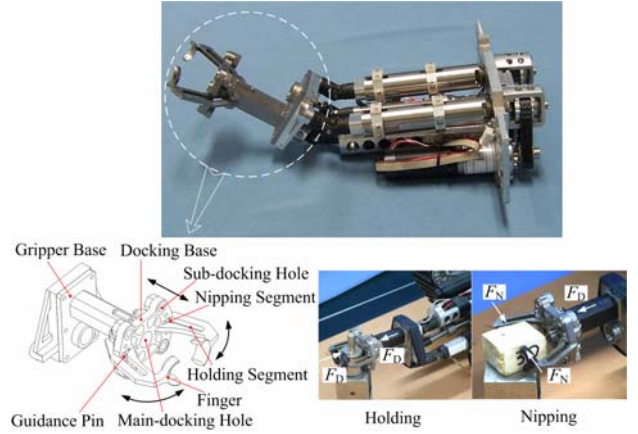


Fig. 3. Docking manipulator and grasping modes

the docking manipulator close to the center of the robot, all of the driving motors are assembled at the opposite side of the gripper. A mechanism with two synchronal belts, two pairs of gears and a slide key mechanism are applied to transfer the output torques of the motors to the two parallel screws and the docking screw respectively.

Fig. 3 shows the realization of the docking manipulator, which can be assembled with the track units by a connecting board. The outline of the fingers and the structure of the Docking base are specially designed to realize two grasping modes, as shown in Fig. 3, as well as the grasping-locking and gradual-alignment docking procedure, which will be explained in sub-section 3.4. The tip of the finger is designed in a half-circle and hook shape to grip the shaft behind the docking disk on the other robot. At the center of the docking base, there is a large cone-shaped hole called main-docking hole; four small cone-shaped holes called sub-docking holes are at the four corners of the docking base. All of these holes will be coupled with the cones on the docking disk of the rotation unit to realize self-alignment and self-constrain.

The cam groove in each finger is divided into two segments: a nipping segment and a holding segment. When the pins are in the nipping segments, they will drive the gripper to open or close as long as the docking base moves backward or forward. In this phase, the gripper may perform a grasping mode called nipping. The fingers revolving around the gripper shafts from  $0^\circ$  -  $24^\circ$  will result in a fluctuating distance between two tips from 2mm - 43mm, which are also the width limits of the object being nipped. The nipping force  $F_N$  is introduced by the pushing force of the docking base  $F_D$ . When the pins enter the holding segments, a holding mode will be performed by the gripper. The available thickness of the objects that can be held is between 1mm to 22mm in theory. The holding force equals  $F_D$ . The value of  $F_D$  and  $F_N$  can be calculated by according to the physical parameters of the docking motor, the gear ratio, the docking screw, and the dimensions of the fingers. The continuous stall value of  $F_D$  is 28.3 kN; and the possible maximum value of  $F_N$  changes from 4.8 kN to 17.3 kN, when the object width changes from 43mm to 2mm.

When grasping, the robots in JL-2 will perform a nipping action for an object with flat surfaces and a holding action for a round object. It seems that the contact forces between the gripper and objects are too large, but those are necessary to ensure a reliable self-alignment and solid connection when docking. Actually, during the grasping and docking phases, the contacting forces will be limited by monitoring the current in the docking motor to protect the object and fingers from being damaged.

### 3.3. Rotation unit

The rotation unit is simply composed of a motor and a docking disk mounted on the output shaft of the motor, as shown in Fig. 4. Two functions will be performed by the rotation units. The first one is to coordinate with the docking manipulator to complete the gradual aligning procedure, which is guaranteed by the shape of the docking disk. The other one is to turn the robot about the Z axis when docked. Therefore, the axis of the rotation unit should pass through point O (as shown in Fig. 2) in the connected state. As mentioned above, the main-docking cone and the sub-docking cones on the docking disk will be coupled with the holes in the docking base to guarantee the self-aligning function and to overcome the rotation load around the Z axis when docked. Two edges of the docking disk are designed in a curve to permit the gripper to encompass the disk easily. The diameter of the shaft behind the disk is less than that of the circle of the finger tip of the docking gripper. As a result, when the gripper catches the shaft, the misalignments between two robots are acceptable to a certain degree. The connection between the gripper and the docking disk should be powerful enough to overcome the loads arising from the weight of the robot. The rotation unit will be supported by a connecting board when assembled on the robot.

### 3.4. Principle of docking

By virtue of the special designs of the docking gripper and the docking disk, the docking procedure is divided into three phases: the approaching phase, grasping phase and locking phase.

When docking, one robot is called the "active robot", if it makes use of its docking manipulator to actively connect another one. On the contrary, the robot waiting to be connected is called the "passive robot". During the approaching phase, the "passive robot" stops moving,

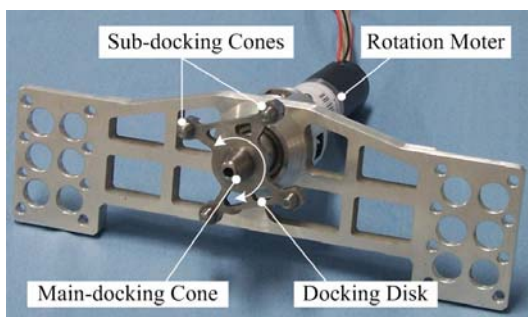


Fig. 4. Realization of the rotation unit

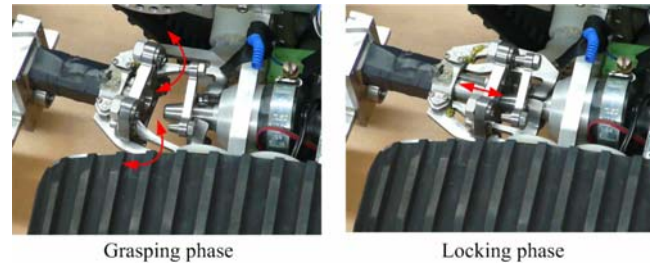


Fig. 5. Two phases in docking procedure

but rotates its docking disk to align with the gripper of the "active robot". The "active robot" opens the gripper completely, and then it keeps moving forward and adjusting the postures of the gripper simultaneously, until the gripper encompasses the docking disk belonging to the "passive robot".

Then the grasping phase begins, during which the gripper closes to diminish the errors in the horizontal plane, namely  $d_y$  and  $\varepsilon_x$ , as shown in Fig. 5. This function is ensured by the contacting forces between the fingers and the docking disk. Although the contacting forces are changing during this procedure, they are powerful enough to overcome the friction force between the tracks and the ground, and will align two robots in the horizontal plane. At the end of the grasping phase, the completely closed gripper not only decreases the  $d_y$  and  $\varepsilon_x$  distinctively, but also grasps the docking disk and prevents it from escaping.

After the grasping phase, the locking phase will be triggered. Here the docking base will be stretched out while the main-docking cone will be embedded in the main-docking hole. This procedure is ensured by their respective dimensions. As soon as the main-docking cone and the main-docking hole make contact, the contacting forces will diminish the aligning errors in the vertical plane, namely  $d_x$  and  $\varepsilon_y$ , as well as the rudimental errors  $d_y$  and  $\varepsilon_x$  in the horizontal plane. At the end of this period, the sub-docking cones will fit the sub-docking holes, eliminating all of the five errors in the end.

After the locking phase, all of the six DOF between two robots are constrained, and the docking disk is held forcefully between the docking base and the gripper by the resident pressure with a maximum value of 28.3KN. Since the driving chain from the docking motor to the gripper and the docking disk is self-locked, there is no possibility to open the gripper and disconnect the two robots, unless the docking motor is controlled to do it.

### 3.5. Kinematics of spherical joint

When the robots connect, JL-2 is able to perform particular motions by virtue of the two motorized spherical joints between them, such as self-recovery, crossing wide trenches, climbing stairs, passing through narrow fences, lateral motion, and etc. These locomotion capabilities will enhance the adaptability of JL-2 to rugged terrains and have been validated by JL-1 (Wang, W.; et al., 2008).

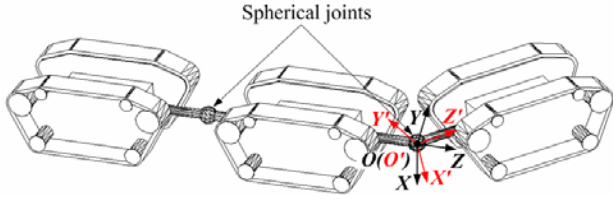


Fig. 6. Spherical joints of JL-2

In Fig. 6, two Cartesian coordinates  $OXYZ$  and  $O'X'Y'Z'$ , whose original points are both located at the center of the spherical joint, coincide with the middle robot and the front robot respectively. Therefore, the posture changing of the robot can be represented by the relative rotation between these two coordinates, which is denoted by a vector  $\theta$  in equation (3). The outputs of the three motors of the spherical joints are denoted by a vector  $q$  in equation (4).

$$\theta = [\theta_x, \theta_y, \theta_z]^T \quad (3)$$

$$q = [\theta_{m1}, \theta_{m2}, \theta_R]^T \quad (4)$$

Where,

$\theta_{m1}$  and  $\theta_{m2}$  are the output angles of two motors driving the parallel mechanism respectively;

$\theta_R$  is the output angle of the rotation motor.

The relationship between  $\theta$  and  $q$  can be denoted by the following equations (5) ~ (7).

$$\theta_{m1} = 2\pi(A-L)/lb \quad (5)$$

$$\theta_{m2} = 2\pi(B-L)/lb \quad (6)$$

$$\theta_R = \theta_z \quad (7)$$

Where,

$$A = [(K(c\theta_x c\theta_z + s\theta_x s\theta_y s\theta_z) - K(-s\theta_z c\theta_y + s\theta_x s\theta_y c\theta_z) + Lc\theta_x s\theta_y - Kc\theta_z - Ks\theta_z)^2 + (K(c\theta_x s\theta_z) - K(c\theta_x c\theta_z) - Ls\theta_x - Ks\theta_z + Kc\theta_z)^2 + (K(-s\theta_y c\theta_z + s\theta_x c\theta_y s\theta_z) - K(s\theta_y s\theta_z + s\theta_x c\theta_y c\theta_z) + Lc\theta_x c\theta_y)^2]^{1/2};$$

$$B = [(K(c\theta_x c\theta_z + s\theta_x s\theta_y s\theta_z) + K(-s\theta_z c\theta_y + s\theta_x s\theta_y c\theta_z) + Lc\theta_x s\theta_y - Kc\theta_z + Ks\theta_z)^2 + (K(c\theta_x s\theta_z) + K(c\theta_x c\theta_z) - Ls\theta_x - Ks\theta_z - Kc\theta_z)^2 + (K(-s\theta_y c\theta_z + s\theta_x c\theta_y s\theta_z) + K(s\theta_y s\theta_z + s\theta_x c\theta_y c\theta_z) + Lc\theta_x c\theta_y)^2]^{1/2};$$

$lb$  is the pitch of the ball screw  $AC$  and  $BD$ ; the other parameters are defined in Fig. 2 and equations (1), (2).

According to equations (5) ~ (7), the controllers can calculate the output angles of the motors to realize the desired posture-adjustment actions.

### 3.6. Workspace analysis of the motorized spherical joints

When the robots connect, JL-2 is able to perform particular motions by virtue of the two motorized spherical joints between them, such as self-recovery, crossing wide trenches, climbing stairs, passing through narrow fences, lateral motion, and etc. These locomotion capabilities will enhance the adaptability of JL-2 to rugged terrains and have been validated by JL-1. According to equations (5) ~ (7) and the structure constraints between two robots, we can acquire the available kinematics workspace of one spherical joint, as shown in Fig. 7. If special joint paths are selected inside this workspace and followed by the joint, JL-2 will perform the above locomotion actions.

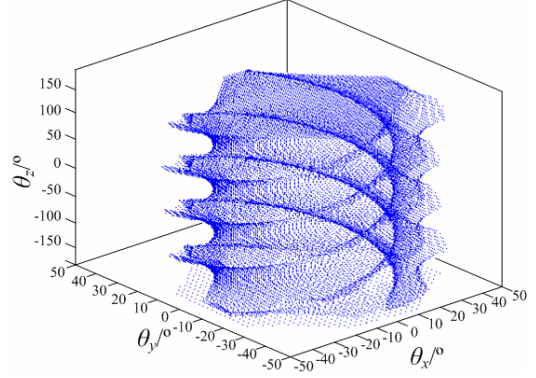


Fig. 7. Available kinematics workspace of the spherical joint

To ensure that every point in the kinematics workspace is reachable, the layout of the three motors should follow equations (8) and (9).

$$\begin{bmatrix} \dot{\theta}_{m1} & \dot{\theta}_{m2} & \dot{\theta}_R \end{bmatrix}^T = J \begin{bmatrix} \dot{\theta}_x & \dot{\theta}_y & \dot{\theta}_z \end{bmatrix}^T \quad (8)$$

$$\begin{bmatrix} M_1 & M_2 & M_R \end{bmatrix}^T = (J^T)^{-1} \begin{bmatrix} M_x & M_y & M_z \end{bmatrix}^T \quad (9)$$

Where,

$J$  is the Jacobian matrix, which is acquired from the differentiation of the equations (5) ~ (7);

$M_1$  and  $M_2$  are the output torques of the two motors of the parallel mechanism;

$M_R$  is the output torques of the rotation motor;

$M_x, M_y$  and  $M_z$  are the loads on the spherical joint.

The loads on the spherical joints arise from the weight of the robots  $G$  and the supporting forces of the ground  $N_G$ , and change when JL-2 adjusts the robots' postures, as shown in Fig. 8. To estimate the continuous stall torque of the spherical joint motors, three typical postures where the  $M_x, M_y$  and  $M_z$  reach their maximum values respectively are illustrated by Fig. 8.

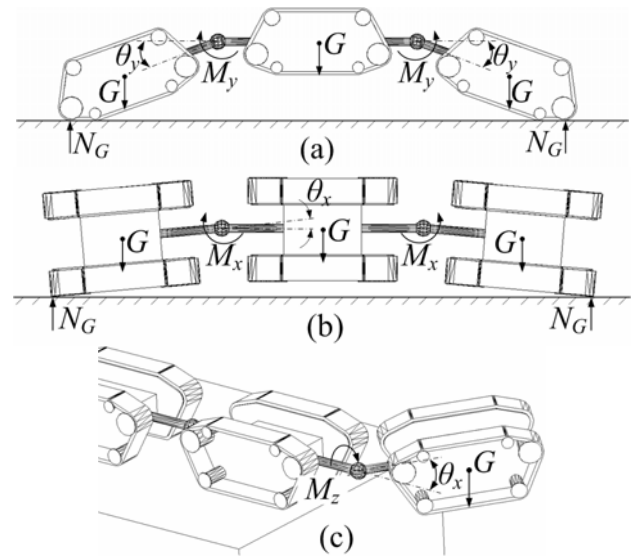


Fig. 8. Three typical postures

In Fig. 8(a), JL-2 is lifting the middle robot by turning the joints about the  $Y$  axes. According to the structure of the robots,  $M_y$  will reach its maximum value when  $\theta_y$  equals  $12^\circ$ . If the weight of one robot is supposed to be 10 kg in the design period, the maximum value of  $M_y$  will equal 23.8Nm in this situation. In Fig. 8(b), JL-2 is turning the joints about the  $X$  axes to lift the middle robot to self-right from the side-over state. When  $\theta_x$  equals  $2.5^\circ$ ,  $M_x$  will reach the maximum value 19.6Nm. In Fig. 8(c), the front robot is supported by the other two robots and is turned about the  $Z$  axis. When  $\theta_x$  and  $\theta_z$  equal  $45^\circ$  and  $0^\circ$  respectively,  $M_z$  will reach the maximum value 4.2Nm. By inserting the above maximum values of  $M_x$ ,  $M_y$  and  $M_z$  into equation (9), we can acquire the necessary output torques of the motors for the spherical joint, by which the layout of these motors can be completed.

#### 4. Control system

##### 4.1. Hardware and sensors for automatic docking

Different cooperation modes are available for JL-2, such as parallel movement or manipulation and physically related reconfiguration. To meet the requirements of the changing cooperation mode, JL-2 adopts a distributed control system as shown in Fig. 9, so that every robot can process the information and performs the motion independently. In this distributed system, a PC with joystick and three robots communicate with each other through a wireless LAN.

Every robot in the JL-2 prototype adopts the same control hardware, which is also shown in Fig. 9. This control hardware is based on the master-slave structure and meets the requirements of functionality, extensibility, and easy handling.

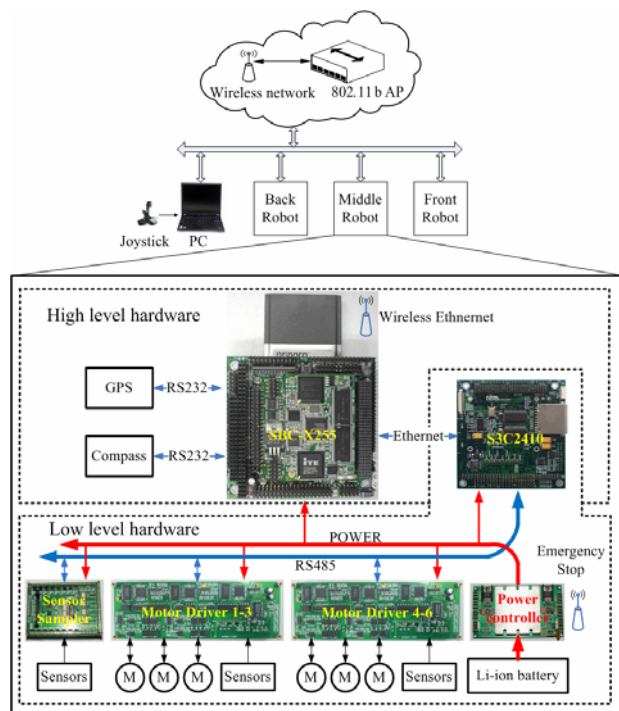


Fig. 9. Hardware of the control system

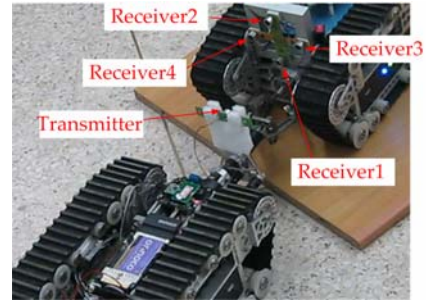


Fig. 10. Sonar sensors for automatic docking

A global and local positioning sensor system is intergrated in JL-2 to realize the automatic docking. Each robot of JL-2 is equipped with a GPS and an electric compass which are responsible for the global positioning in a large area. However, the positioning accuracy of GPS is normally no better than 0.2m, and does not meet the requirement of the docking action. Therefore, a sonar based inter-robot docking guidance system is designed to guide the robots to diminish the position and orientation errors among them, as shown in Fig. 10.

This sonar guidance system is composed of one transmitter which is centrally installed on one robot, and four receivers symmetrically installed on the other robot. When docking, two robots firstly approach each other by following the position and oritation data of the GPS and compass sensors. As soon as the distance between the robots is less than 0.5m, which is the maximum detectable distance of the sonar system, the two robots will start the sonar system and rotate in different speeds to ensure that the receivers capture the ultrasonic signal sent by the transmitter. In theory, the intensity of the received signal is linear to the distance between the transmitter and the receiver. By comparing the signal intensities of the two horizontally arranged receivers and the two vertically arranged recerviers respectively, we will acquire the horizontal and vertical aligning errors between two robots. The oritation of the robots will be adjusted to diminish the signal differences between the receivers. Then, two robots will approach each other and adjust their oritation repeatedly according to the sensor data, until the docking disk is surrounded by the docking gripper. At last, the controller triggers the final grasping action described in 3.4.

The detailed discussion of this sonar guidance system can be found in our previous paper (Li, D.Z.; et al., 2008).

##### 4.2. Software architecture

To cope with the distributed hardware and the changing cooperation modes, the software architecture of JL-2 is based on a multi-agent behavior-based structure and a multi-threaded programming methodology. The architecture shown in Fig. 11 includes a master serving as a global path planner and several slaves executing the commands from the master. Depending on the requirements of the tasks, each robot could be a master or a slave.

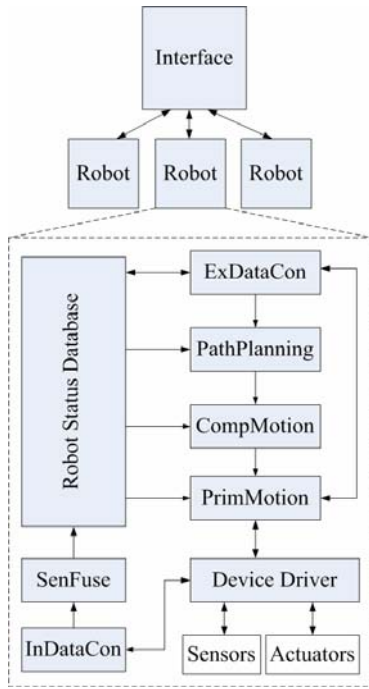


Fig. 11. Software architecture

To handle different hardware requests simultaneously and compute in real-time, the multi-task software is built in the SBC-X255 and the S3C2410 based on the Embedded Linux Operation System. The *ExDataCon* thread provides the data communication between robots and user interface; the *InDataCon* thread takes charge of receiving data or sending commands to the inner-devices; the *SenFuse* and *PathPlanning* threads process the sensor data, construct a local map and generate a feasible path, and the *CompMotion* thread deals with the composite behaviors composed of several primitive motions such as “Forward” and “Turning around”, which are controlled by the *PrimMotion* thread. The communication threads, *ExDataCon* and *InDataCon*, maintain the *Robot Status Database* which records all of the information. As a result, the reconfiguring action can be implemented efficiently and harmoniously according to the global information saved in the system status database. Actually, every robot and the interface have one copy of the *Robot Status Database* in their memory. Therefore, the *Robot Status Database* is a common “Blackboard” being accessible for every node in the JL-2 control system.

Once the global tasks, such as “Docking”, “Undocking”, “90° recovery”, “Whole turning left”, etc., are sent by the user through the interface on the PC, one robot is chosen to be a master according to its role in the task, and then the master generates a set of composite motions based on the task and the status of all robots. For example, when the “90° recovery” task is sent out, the middle robot is chosen to be the master, since it will control the two spherical joints simultaneously. Afterwards, every composite motion is transmitted to the appropriate robot by the *ExDataCon* thread. At last, the composite motions are decomposed and sent to the *PrimMotion* thread to achieve the desirable motions.



Fig. 12. Grasping experiments

## 5. Experiments

A series of experiments have been executed to test the basic functions of the JL-2 prototype. To date, some actions can be automatically performed by JL-2, such as posture-adjusting actions and automatic docking. However, due to the absence of intelligent objects and/or terrains recognition technologies, the manual control is still necessary for JL-2 to perform the navigation and grasping action in the field. That means JL-2 is a semi-automatic robotic system at present.

### 5.1. Grasping

Fig. 12 shows the grasping tests. Two grasping modes have been tested on the middle robot and the back robot. In the experiments, the gripper successfully nipped several wood blocks. To grasp a round object, the holding mode was applied. If being operated carefully, the robot can even grasp a pingpong.

### 5.2. Docking

To test the self-aligning abilities of the docking mechanism, the five posture errors,  $d_x$ ,  $d_y$ ,  $\varepsilon_x$ ,  $\varepsilon_y$ , and  $\varepsilon_z$ , were preset individually in several experiments. Fig. 13 shows the four docking experiments, in which the photos above the arrows present the states before docking, and the others below the arrows show the docked states. Since the posture error  $\varepsilon_z$  between two robots can be diminished by the rotation motor, the docking procedure to overcome  $\varepsilon_z$  is relatively simple and not shown at here. According to these experiments, we can find that when horizontal errors  $\varepsilon_x$  and  $d_y$  are involved, the docking mechanism only needs to overcome the friction force between the tracks and the ground, but with vertical errors  $\varepsilon_y$  and  $d_x$ , the weight of the robot has to be overcome. As a result, the docking ability of JL-2 in the horizontal plane is better than that in the vertical plane.

The self-aligning ability around the Z axis is the poorest one, because the multi sub-cones can cause over-constraint, although they will help to realize a solid connection. It is not a serious problem in actual docking actions, as the rotation angle of the docking disk can be accurately adjusted by the rotation motor.

When docked, a very solid connection is ensured by the high pressure and the multi-point mating structure between the docking base and disk. Such a connection without any gap between connected parts enables the posture-adjusting experiments.

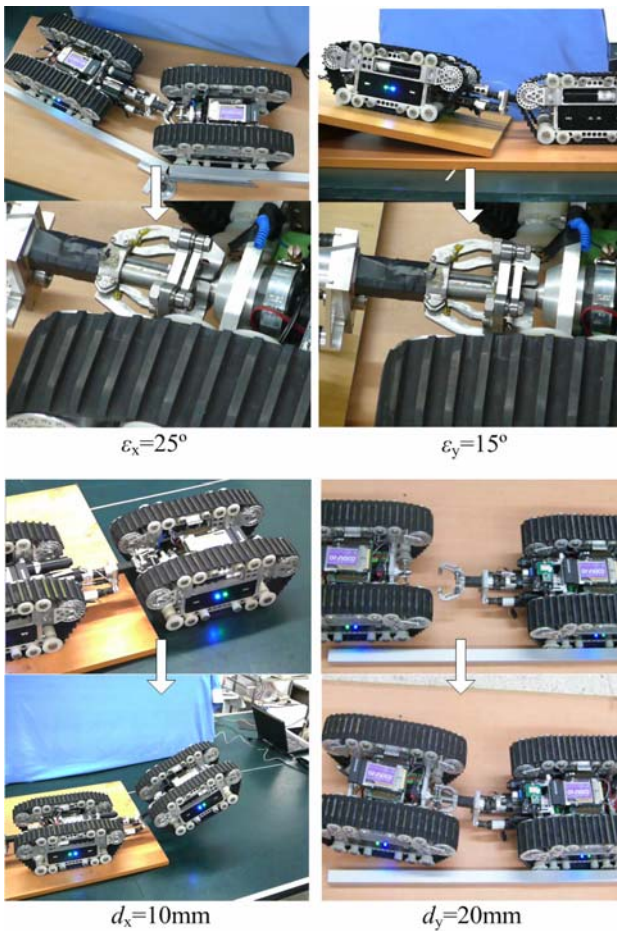


Fig. 13. Docking experiments



Fig. 14. 90° self recovery

However, the multi-point mating structure introduces the over-constraint phenomena between the docking base and disk, and limits the further improvement of the self-aligning capability.

Besides the above experiments testing the docking limits, the automatic docking actions are also performed. According to our experiments, the robots in JL-2 are able to finish the docking actions successfully if the distance between them is less than the detectable distance (0.5m) of the sonar guidance system.

### 5.3. Posture adjusting

JL-2 performed similar posture-adjusting experiments to JL-1, such as self recovery, lateral motion, passing through a narrow fence, and so on. Because JL-2 shares the same principle with JL-1 when performing the posture-adjusting actions, only the 90° self recovery experiment is shown in Fig. 14 as an example. The detailed discussion can be found in our previous paper (Wang, W.; et al., 2008).

The results of our experiments are listed in Table 1.

Item	Values	
<b>Physical parameters of single robot</b>		
Weight	Front robot	7.2kg
	Middle robot	9.1kg
	Back robot	8.5kg
Dimensions	Front robot	370*252*172mm <sup>3</sup>
	Middle robot	569*252*172mm <sup>3</sup>
	Back robot	569*252*172mm <sup>3</sup>
Maximum moving velocity		200 mm/s
Maximum endurance time		2 hour
<b>Grasping ability</b>		
Pitching angle		-45°~+45°
Yawing angle		-42°~+42°
Object width in nipping mode		5-30mm
Object diameter in holding mode		5-20mm
Rating nipping force		0.65-0.88kN
Rating holding force		10.1kN
<b>Docking ability (Maximum permitted errors )</b>		
Horizontal position error $d_y$		-30~+30mm
Horizontal orientation error $\varepsilon_x$		-35~+35°
Vertical position error $d_x$		-15~+15mm
Vertical orientation error $\varepsilon_y$		-20~+20°
Rotation error $\varepsilon_z$		-8~+8°
<b>Posture adjusting ability</b>		
Turning angle around X-axis $\theta_x$		-45~+45°
Turning angle around Y-axis $\theta_y$		-42~+42°
Turning angle around Z-axis $\theta_z$		-180~+180°
Maximum torque around X-axis $M_x$		20.5Nm
Maximum torque around Y-axis $M_y$		24.5Nm
Maximum torque around Z-axis $M_z$		4.5Nm

Table 1. Basic performance specifications

## 6. Conclusions

This paper presents the design and realization of JL-2, a new version of the JL series reconfigurable mobile robot system, which is distinguished from its predecessor JL-1 by a docking manipulator and a 3D docking ability. The analyses and tests yield the following conclusions.

1. Integrating a simple gripper at the end of the parallel mechanism is a feasible solution to combine the grasping and docking function on reconfigurable mobile robots.
2. The docking ability of JL-2 is enhanced by a 3 DOFs docking gripper and the high docking forces arising from a cam guidance mechanism. It is possible for JL-2 to realize the docking action in rugged terrains in the future.
3. Although the multi-point mating structure ensures a solid connection, it may introduce an over-constraints problem which results in a poor self-aligning ability around the rotation axis.

Currently, the robots in the JL-2 system only performed some typical experiments to testify their basic performances respectively. Though the capabilities of JL-2 can be reflected in these experiments partially, the real

testimonies on the tough field are necessary to validate the robustness of JL-2. Before the JL-2 system can be really applied on the field for the rescuing and detecting tasks, the future work should include improving the gripper and the docking disk to further enhance the docking ability, designing the dust and water proof covers, developing intelligent objects and terrains recognition technology, and etc. Besides, the grasping trajectory plan of JL-2 in docked state is also an open question in the future work.

## 7. Acknowledgment

This project is supported by the National High-tech R&D Program (863 Program) of China (No. 2006AA04Z241). The authors appreciate the hard work of Jie Xia, Hualei Fu, Xiongfeng Li and Zongliang Li for this project.

## 8. References

- Borenstein, J.; Hansen, M. & Borrell, A. (2007). The OmniTread OT-4 serpentine robot – design and performance, *Journal of Field Robotics*, Vol. 24, No. 7, pp. 601-621
- Brown, H. B.; Weghe, J. M. V.; Bererton, C. A. & Khosla, P. K. (2002). Millibot trains for enhanced mobility, *IEEE/ASME Transactions on Mechantronics*, Vol. 7, No. 2, pp. 452-461
- Casper, J. & Murphy, R. R. (2000). Issues in intelligent robots for search and rescue, *SPIE Ground Vehicle Technology II*, 2000
- Estier, T.; Crausaz, Y.; Merminod, B.; Lauria, M.; Piguët, R. & Siegwart, R. (2000). An innovative space rover with extended climbing abilities, *Proceedings of 2000 Space and Robotics*, Albuquerque, New Mexico, Feb. 2000
- Gilpin, K.; Kotay, K.; Rus, D. & Vasilescu, I. (2008). Miche: modular shape formation by self-disassembly, *International Journal of Robotics Research*, Vol. 27, No. 3-4, pp. 345-372
- Gross, R.; Tuci, E.; Dorigo, M.; Bonani, M. & Mondada, F. (2006). Object transport by modular robots that self-assemble, *Proceedings of the IEEE International Conference on Robotics and Automation*, Orlando, Florida, U.S.A., May 2006, pp. 2558-2564
- Haraguchi, R.; Osuka, K.; Makita, S. & Tadokoro, S. (2005). The development of the mobile inspection robot for rescue activity MOIRA2, *Proceedings of 12th International Conference on Advanced Robotics*, Seattle, U.S.A., July 2005, pp. 498-505
- Hirose, S. & Morishima, A. (1990). Design and control of a mobile robot with an articulated body, *International Journal of Robotics Research*, Vol. 9, No. 2, April 1990, pp. 99-113
- Hirose, S.; Shirasu, T. & Fukushima, F. E. (1996). A proposal for cooperative robot “Gunryu” composed of autonomous segments, *Proceedings of the IEEE/RSJ/GI International Conference on Robotics and Autonomous Systems*, Munich, Germany, Nov. 1996, pp. 1532-1538
- Kawakami, A.; Torii, A.; Motomura, K. & Hirose, S. (2002). SMC rover: planetary rover with transformable wheels, *Proceedings of the 41st SICE Annual Conference*, Nanjing, China, Aug. 2002, pp. 157-162
- Kawauchi, Y.; Inaba, M. & Fukuda, T. (1994). Dynamically Reconfigurable intelligent system of cellular robotic system (CEBOT) with entropy min/max hybrid algorithm, *Proceedings of the IEEE International Conference on Robotics and Automation*, San Diego, C.A., U.S.A., May 1994, pp. 464-469
- Li, D.Z.; Fu, H.L. & Wang, W. (2008). Ultrasonic based autonomous docking on plane for mobile robot, *Proceedings of the IEEE International Conference on Automation and Logistics*, Qingdao, China, Sept. 2008, pp. 1396-1401
- Lu, Z. L.; Ma, S. G.; Li, B. & Wang, Y. C. (2006). 3D locomotion of a snake-like robot controlled by cyclic inhibitory CPG model, *Proceedings of the 2006 IEEE/RSJ International Conference on Intelligent Robots and Systems*, Beijing, China, October 2006, pp. 3897-3902
- Masam, A.; Takayama, T. & Hirose, S. (2004). Development of “Souryu-III”: connected crawler vehicle for inspection inside narrow and winding spaces, *Proceedings of the 2004 IEEE/RSJ International Conference on intelligent Robots and Systems*, Sendai, Japan, Sept. 2004, pp. 52-57
- Matthies, L.; Xiong, Y.; Hogg, R.; Zhu, D.; Rankin, A.; Kennedy, B.; Hebert, M.; Maclachlan, R.; Won, C.; Frost, T.; Sukhatme, G.; McHenry, M. & Goldberg, S. (2002). A portable, autonomous, urban reconnaissance robot. *Robotics and Autonomous Systems*, Vol. 40, No. 2-3, Aug. 2002, pp. 163-172
- Mondada, F.; Guignard, A.; Bonani, M.; Bar, D.; Lauria, M. & Floreano, D. (2003). SWARM-BOT: from concept to implementation, *Proceedings of the 2003 IEEE/RSJ International Conference on Intelligent Robotics and Systems*, Las Vegas, Nevada, USA, Oct. 2003, pp. 1626-1631
- Mondada, F.; Bonani, M.; Magnenat, S.; Guignard, A. & Floreano, D. (2004). Physical connections and cooperation in swarm robotics, *Proceedings of 8th Conference on Intelligent Autonomous Systems*, Amsterdam, Holland, March 2004, pp. 53-60
- Mori, M. & Hirose, S. (2002). Three-dimensional serpentine motion and lateral rolling by active cord mechanism ACM-R3, *Proceedings of the 2002 IEEE/RSJ International Conference on Intelligent Robots and Systems*, EPL, Lausanne, Switzerland, October, 2002, pp. 829-834
- Murata, S.; Yoshida, E.; Kamimura, A.; Kurokawa, H.; Tomita, K. & Kokaji, S. (2002). M-tran: self-reconfigurable modular robotic system, *IEEE/ASME*

- Transactions on Mechatronics, Vol. 7, No. 4, pp. 431-441
- Murphy, R.R. (2000). Marsupial and shape-shifting robots for urban search and rescue. *IEEE Intelligent Systems and their applications*, Vol. 15., No. 2, March-April 2000, pp. 14-19
- Nilsson, M. (2002). Heavy duty connectors for self-reconfiguring robots, *Proceedings of the IEEE International Conference on Robotics and Automation*, Washington, D.C., U.S.A., May 2002, pp. 4071-4076
- Sproewitz, A.; Asadpour, M.; Bourquin, Y. & Ijspeert, A. J. (2008). An active connection mechanism for modular self-reconfigurable robotic systems based on physical latching, *Proceedings of the IEEE International Conference on Robotics and Automation*, Pasadena, C.A., U.S.A., May 2008, pp. 3508-3513
- Tokuda, K.; Osuka, K. & Ono, T. (1999). Concept and development of general rescue robot CUL, *Proceedings of the IEEE/RSJ International Conference Robotics and Autonomous Systems*, Kyongju, Korea, Oct. 1999, pp. 1902-1907
- Visentin, G.; Van Winnendael, M. & Putz, P. (2001). Advanced mechatronics in ESA space robotics developments, *Proceedings of the 2001 IEEE/RSJ International Conference on Intelligent Robots and Systems*, Maui, Hawaii, USA, Oct. 2001, pp. 1261-1266
- Wang, W.; Zhang, H. X.; Zhang, J. W. & Zong, G. H. (2008). Force cooperation in a reconfigurable field multi-robot system, *Journal of Field Robotics*, Vol. 25, No. 11-12, pp 922-938
- Yim, M.; Shen, W. M.; Salemi, B.; Rus, D.; Moll, M.; Lipson, H.; Klavins E. & Chirikjian. G. S. (2007). Modular self-reconfigurable robot Systems, *IEEE Robotics and Automation Magazine*, Vol. 14, No. 1, pp. 43-52
- Zhang, H. X.; Wang, W.; Deng, Z. C. & Zong, G. H. (2006). A novel reconfigurable robot for urban search and rescue, *International Journal of Advanced Robotic Systems*, Vol. 3, No. 10, pp. 359-366
- Zykov, V.; Mytilinaios, E.; Adams, B. & Lipson, H. (2005). Self-reproducing Machines, *Nature*, Vol. 435, No. 7038, pp. 163-164